



ASME Accepted Manuscript Repository

Institutional Repository Cover Sheet

Cranfield Collection of E-Research - CERES

ASME Paper

Title: Evaluation of Extreme Value Predictions for Unsteady Flow Distortion of Aero-Engine Intakes

Authors: Matteo Migliorini, Pavlos K. Zachos, David G. MacManus

ASME Journal

Title: Journal of Engineering for Gas Turbines and Power

Volume/Issue: Volume 146, Issue 9

Date of Publication (VOR* Online): _11 March 2024_

ASME Digital Collection URL: <https://asmedigitalcollection.asme.org/gasturbinespower/article-abstract/doi/10.1115/1.4064728/1197094/Evaluation-of-Extreme-Value-Predictions-for>

DOI: 10.1115/1.4064728

*VOR (version of record)

Evaluation of extreme value predictions for unsteady flow distortion of aero-engine intakes

Matteo Migliorini*, Pavlos K. Zachos, David G. MacManus

Centre for Propulsion and Thermal Power Engineering, Cranfield University, Cranfield, Bedfordshire, MK43 0AL, UK

*Corresponding author. Email: matteo.migliorini@cranfield.ac.uk

Abstract

Unsteady flow distortion is of interest for the development air-breathing propulsion systems. Stochastic fluctuations can generate incompatibilities between intakes and aero-engines. Observing the extreme flow distortion events during experimental testing is not guaranteed and statistical models such as Extreme Value Theory (EVT) can be used to estimate the occurrence and magnitude of the fluctuations. However, the current industry standard does not provide guidance on how to apply these methods to obtain useful predictions. This work proposes a systematic process to assess the required number of observations for obtaining statistical convergence of the EVT predictions. This is achieved through shuffling of the data samples and relies on the availability of a sufficiently large initial dataset. This can be adopted by gas turbine engineers to evaluate the data recording requirements and to potentially reduce costs associated with experimental programs.

Nomenclature

A	=	Area, m ²
AIP	=	Aerodynamic Interface Plane
AIR	=	Aerospace Information Report
CI	=	confidence interval for the EVT model
cov	=	covariance
D_{in}	=	diameter at the inlet of the S-duct, mm
EVT	=	Extreme Value Theory
f_s	=	sampling frequency, Hz
k	=	number of exceedances
SAE	=	Society of Automotive Engineers
SI	=	Swirl Intensity (SAE), °
SS	=	Sector Swirl (SAE), °
std	=	standard deviation
U_b	=	upper bound of the EVT model
V	=	velocity component, m/s
var	=	variance
α	=	absolute swirl angle, °, $\tan^{-1}(v_\theta/v_z)$
μ	=	exceedances threshold, °
ξ	=	shape parameter of the EVT model
σ	=	scale parameter of the EVT model

1. Introduction

For aero-engines the evaluation of the maximum expected flow distortion is a key parameter to assess the compatibility between air induction systems and propulsion systems [1]. Stochastic flow disturbances with relatively

large magnitudes could adversely affect the operation of an aero-engine and thus could affect its stability and mechanical compatibility [2,3]. For example, peak distortion events generate instabilities which can trigger spike-stall inception [4]. Thus, the compatibility between the intake and propulsion system is affected by the peak distortion levels that the aero-engine can tolerate [5]. Consequently, to reduce the risk carried to final verification tests, is it important to estimate during initial development phase the maximum expected distortion levels.

Although the peak distortion may be observed during experimental testing, due to its random nature this is not guaranteed [6]. Extreme Value Theory (EVT) has been used to model the extremes of the distribution of dynamic and stochastic variables and to estimate the peak values and associated probability. In the field of flow distortion, these methods were first considered by Jacocks and Kneile [7] and more recently have been applied to pressure and swirl distortion in S-duct diffusers [8,9]. The EVT approach offers potential benefits for estimating peak distortion levels in intake-engine integration assessments where otherwise the observation of the peak distortion would result in time-consuming and expensive experimental or computational campaigns. Potential benefits of these estimation techniques are acknowledged by the industry standard on intake flow distortion as reported in SAE AIR 5826B [10]. However, this standard simply refers to the potential benefits and does not provide an established best practice or guidelines on how to apply the methods beyond that reported by Jacocks and Kneile [7]. Within that context of the state of the art, the contribution of this work is to propose a methodology to systematically apply EVT methods to determine minimum data sizes needed to identify peak distortion events.

Recently, extreme value statistics have been applied for the prediction of maximum swirl distortion levels based on Particle Image Velocimetry (PIV) measurements at the exit of an S-duct diffuser [9]. The PIV measurements provide considerable advantages in synchronous spatial and temporal resolution compared with the conventional methods. The experimental testing time was chosen to ensure convergence mean and standard deviation of the 3D velocity components. However, the required number of observations for statistical convergence of the extreme values such as peak distortion events had not been assessed. In the perspective of the application to EVT methods for product development and validation, and for a rational use of resources, it is fundamental to determine the required test duration for useful EVT predictions. This paper proposes a systematic method to estimate the required experimental measurement samples to enable the prediction of extreme values. The evaluation is based on random subsets generated through shuffling of the measured dataset.

2. Methods

The unsteady swirl distortion data used in this work was obtained with Time-Resolved Particle Image Velocimetry measurements at the exit plane of an S-duct diffuser, located $0.5 D_{in}$ downstream of the S-duct outlet plane. The experimental setup is reported in Zachos et. al [11] and the aerodynamics operating point was Mach 0.27 at the S-duct inlet reference plane. Details of the measurement arrangement are reported in Migliorini et. al [9]. The PIV data was acquired at a frequency of 8kHz, which is about 10 times greater than the highest dominant flow frequency. 200,000 synchronous measurements of the 3 velocity components were acquired at the duct exit. The swirl angle is computed from the tangential velocity (V_θ) and the out-of-plane velocity (V_z) (Eq. 1) and it is assumed positive in the counter-clockwise direction when the measurement plane is viewed from downstream. The swirl distortion has been assessed with the Swirl Intensity (SI) metric by SAE International [12]. This is computed with the integral of the positive and negative sector swirls (SS^+ , SS^-) in the circumferential extents (θ) of the ring i of a polar grid with i rings and j rakes (Eq. 2).

$$\alpha = \arctan\left(\frac{V_\theta}{V_z}\right) \quad (1)$$

$$SI(i) = \frac{\sum_{k=1}^m SS_{i,k}^+ \cdot \theta_{i,k}^+ + \sum_{k=1}^m |SS_{i,k}^-| \cdot \theta_{i,k}^-}{360} \quad (2)$$

The Extreme Value Theory method [6] was used to predict the maximum swirl intensity (SI) distortion levels beyond the experimental observations. This work used the Peak-Over-Threshold formulation by Coles [6], which classifies the events as extreme on the condition they exceed a threshold μ . If this threshold is sufficiently large and the

number of observations, n , is also sufficient, the limit distribution of the k excesses Y_i (Eq. 3) tends to a Generalized Pareto Distribution (Eq. 4). The shape ξ and the scale σ are parameters of this distribution. An upper bound $U_b = \mu - \frac{\sigma}{\xi}$ exists and limits the distribution of the k excesses on the condition that the shape factor is $\xi < 0$. Appropriate choice of the shape ξ and the scale σ parameters can be found by maximizing the logarithmic likelihood function (Eq. 5) [6]. This enables the modelling of the probability of extreme values x_m exceeding the threshold $\zeta_u = \frac{k}{n}$ on average once every m observation (Eq. 6). The application of the delta method yields the error of the extreme value x_m (Eq. 7). This is computed with the product of the gradient ∇x_m (Eq. 8) and the matrix of the variance-covariance VC (Eq. 9). The variance errors of the parameters ζ_u , σ and ξ , whose variance is in turn obtained from the analytical solutions of the model parameters (Eq. 10-13), is contained in the VC matrix (Eq. 9). The uncertainty of the predictions is estimated with a 95% confidence interval CI on the assumption that x_m follows a normal distribution and considering a quantile $z_{\alpha/2} = 1.96$ (Eq. 13). The threshold for the EVT model has been chosen based on the value that minimizes the RMS fit error of the log-likelihood function (Eq. 5) for modelling the exceedances Y_i (Eq. 3). the Peak Over Threshold is one of the possible formulations of the EVT model and alternative formulations are discussed by Coles [6].

$$Y_i = (X_i - \mu) | X_i > \mu \quad (3)$$

$$H(y) = P\{Y \leq y\} = 1 - \left(1 + \frac{\xi y}{\sigma}\right)^{-1/\xi} \quad (4)$$

$$l(\xi, \sigma) = \sum_{i=1}^k \log \left(\frac{dH}{dy}(Y_i, \sigma, \xi) \right) = -k \log(\sigma) - (1 + 1/\xi) \sum_{i=1}^k \log \left(1 + \frac{\xi Y_i}{\sigma} \right) \quad (5)$$

$$x_m = \mu + \frac{\sigma}{\xi} [(m\zeta_u)^\xi - 1] \quad (6)$$

$$\text{var}(x_m) = \nabla x_m^T VC \nabla x_m \quad (7)$$

$$\nabla x_m^T = \left[\frac{\partial x_m}{\partial \zeta_u}, \frac{\partial x_m}{\partial \sigma}, \frac{\partial x_m}{\partial \xi} \right] \quad (8)$$

$$VC = \begin{bmatrix} \text{var}(\zeta_u) & 0 & 0 \\ 0 & \text{var}(\sigma) & \text{cov}(\xi, \sigma) \\ 0 & \text{cov}(\xi, \sigma) & \text{var}(\xi) \end{bmatrix} \quad (9)$$

$$\text{var}(\zeta_u) = \zeta_u(1 - \zeta_u)/n \quad (10)$$

$$\text{var}(\xi) = (1 + \xi)^2/k \quad (11)$$

$$\text{var}(\sigma) = 2(1 + \xi)\sigma^2/k \quad (12)$$

$$\text{cov}(\xi, \sigma) = -(1 + \xi)\sigma/k \quad (13)$$

$$CI = x_m \pm z_{\alpha/2} \sqrt{\text{var}(x_m)} \quad (14)$$

3. Results

In S-duct intakes, the flow distortion is generated inherently in the duct [8,9]. The flow distortion is naturally unsteady due to the interaction between the secondary flow which develop downstream of the S-duct first bend and the flow separation which arises due to the adverse pressure gradient in the diffusing geometry [11]. This generates unsteady total pressure and swirl distortion which has been assessed with metrics defined by SAE International to describe the potency, topology and unsteady fluctuations of the flow distortion [8,9]. Previous work showed that the inherent flow distortion of S-duct intakes is unsteady and that inlet conditions such the ingestion of thick total pressure profiles or vortices as well as the S-duct geometry have an impact on the distribution of extreme distortion events [8,9]. The nature of the distortion and its characteristics have been assessed in computational and experimental work through the analysis of the standard SAE distortion descriptors and unsteady analysis in previous work [13–15].

A population of 200,000 unsteady flow fields has been considered for this study. Out of this data, the area-averaged swirl intensity (\overline{SI}) was extracted as the metric of interest. In this population, a maximum of $\overline{SI}_{peak,exp} = 15.0^\circ$ was measured, and this was taken as a reference value by which to assess the statistical convergence of the extreme

value prediction. In the hypothesis that only limited number of observations are available due to experimental constraints, EVT models can be used to estimate the maximum distortion levels beyond the available observations. To simulate this, a reduced number of samples was extracted from the initial population by considering 2, 5, 10, 20, 40, 60, 100 and 140 X 10³ samples equally spaced in time. The EVT method was used to predict the maximum $\overline{SI}_{peak,EVT}$ for a return period of $m = 2 \times 10^5$ so this could be compared with the measured maximum of the total population (Fig. 1). It is highlighted that in these data subsets, the sampling of the data is of a high enough frequency to resolve in time the fluctuations of swirl intensity of interest of the S-duct flow distortion. Indeed, for the smallest dataset (2,000 samples) and considering the acquisition frequency of 8 kHz, it is possible to capture at least two periods of an 8 Hz oscillation and resolve fluctuations up to 3.125 kHz according to the Nyquist criterion. Thus, this is adequate to cover the range of typical swirl angle fluctuations in these S-duct diffusers [9].

The EVT models derived from datasets with reduced number of samples between 2 and 140 thousand samples predict \overline{SI}_{EVT} with a certain confidence interval CI (Fig. 1). As expected, and in agreement with Coles [6], the EVT models predict a $\overline{SI}_{peak,m=2 \times 10^5}$ and U_b which broadly increases when more samples are considered. The predictions are associated to a certain confidence interval CI which reduces for the models based on more samples. For example, the confidence interval for the EVT model with 20 thousands samples is about $\pm 0.5^\circ$ while for the model with 140 thousand samples it reduces to $\pm 0.2^\circ$. Nevertheless, all EVT models slightly underpredict the peak distortion levels. Among the models, the EVT predicted $\overline{SI}_{peak,m=2 \times 10^5}$ is between 0.3° and 1.3° lower than the measured maximum distortion $\overline{SI}_{peak,exp} = 15.0^\circ$. Evaluating the accuracy of these predictions is not straightforward. For example, the model with 2,000 samples, produces an estimate of $\overline{SI}_{peak,m=2 \times 10^5}$ which is 1.4° degrees lower relative to the observed distortion $\overline{SI}_{peak,exp} = 15.0^\circ$. The usefulness of this prediction can be considered acceptable or not depending on the specific application and the envisaged impact of SI on the compressor surge margin [16]. However, there is a need to establish a systematic method to guide the assessment that is not linked with a specific application, but rather based on statistics.

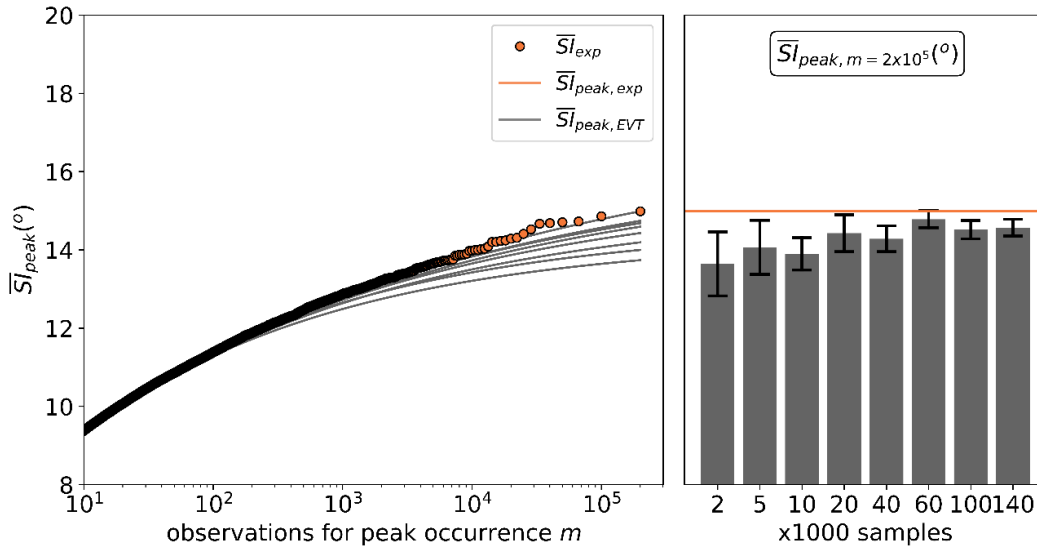


Fig. 1: Statistical convergence of EVT prediction of $\overline{SI}_{peak,m=2 \times 10^5}$ and associated confidence intervals CI compared with measured distortion \overline{SI}_{exp} .

A key consideration is that the convergence of the EVT predictions for increasing number of sample is not monotonic. The variability of the extreme value predictions is attributed to the intrinsic stochastic nature of distortion events with varying levels of swirl intensity \overline{SI} . The accuracy of the $\overline{SI}_{peak,m=2 \times 10^5}$ prediction is strictly related to the number and magnitude of the extreme values which occur within the sample. These are not known a priori. For example, this is illustrated by splitting the original dataset into 10 subsets with 20 thousand samples each and by

using these subsets to model the extreme values (Fig. 2). The projected extreme values of $\overline{SI}_{peak, m=2 \times 10^5}$ range between 13.9 and 15.9°. In previous work, the accuracy of the predictions was assessed with the confidence interval CI [6]. In this example, this varies between $\pm 0.4^\circ$ and $\pm 1.1^\circ$ among the datasets (Fig. 2). However, the CI contains multiple sources of error which include the choice of the threshold, the scale and shape parameter of the EVT model, but also the number of exceedances and number of samples, and it is not clear how this can be used to assess the accuracy of the EVT model. Moreover, in this case, the EVT model which produces an outlier (dataset 7, Fig. 2) is the one with the lowest associated CI. Thus, it is not possible to use this metric to compare EVT results and discern the most accurate.

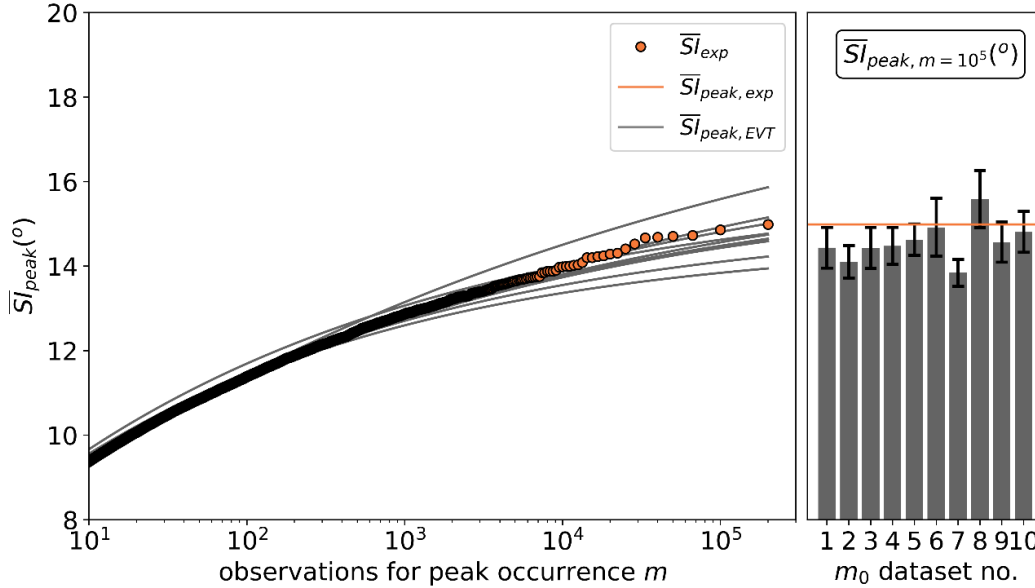


Fig. 2: EVT prediction of $\overline{SI}_{peak, m=2 \times 10^5}$ and associated confidence intervals CI for subsets of the original dataset and comparison with measured distortion \overline{SI}_{exp} .

It is inferred that a systematic and statistical assessment is needed to evaluate the minimum number of experimental observations to produce reliable estimates of the extreme values of the swirl distortion events. A Monte-Carlo shuffling method has been applied to the entire population to produce a random sample from which subsets are extracted. The method of shuffling and the number of shuffling iterations determines the randomness of a sample. In Bayer and Diaconis [17] card probability theory, the randomness is linked with the chances of having any arrangements of the samples with reference to the original series. In a dovetail card shuffle, which consists in cutting the deck cards in half and then riffing the two halves together, they demonstrated that randomness is approached for a number of shuffling iterations greater than $3/2 \log_2 n$, where n is the number of samples [17]. This dovetail shuffling method was thus adopted to shuffle the experimental dataset of this study and obtain new dataset which approach randomness. The experimental dataset was split in half and each of these halves have been riffled together numerically. Since the dataset contains $n = 2 \times 10^5$ samples, randomness approaches a minimum of $3/2 \log_2 n \approx 18$ iterations.

The availability of new arrangements of the experimental dataset enables the development of EVT models based on subsets of the original experimental dataset and to assess the distribution of the $\overline{SI}_{peak, m=2 \times 10^5}$ predictions. From the considerations above, the 18th shuffling iteration and all the subsequent ones are considered as nominally random in accordance to the Bayer and Diaconis definition [17]. For this study, 1,000 random samples not equispaced in time have been considered. Subsets with 2, 5, 10, 20, 40, 60, 100 and 140 $\times 10^3$ samples have been used to derive 1'000 EVT models for each dataset length and to evaluate statistically the predictions. The distribution of the predictions among the 1,000 EVT models as a function of the selected number of samples are shown with letter-value plots [18] (Fig. 3) which are used to highlight the statistical distribution across the full range. As expected, when considering relatively few samples, the $\overline{SI}_{peak, m=2 \times 10^5}$ predictions span across a relative wide range. For

example, for 2'000 samples, the EVT models predict a $\overline{SI}_{peak,m=2 \times 10^5}$ between 12.4° and 18.5°, with a median value of 14.4°. The range of predictions can vary up to approximately $\pm 30\%$ of the median value and therefore these predictions are considered relatively uncertain. The range of $\overline{SI}_{peak,m=2 \times 10^5}$ predictions sharply decreases when EVT is modelled on subsets with a larger number of samples. For example, the range of $\overline{SI}_{peak,m=2 \times 10^5}$ reduces from [12.4°, 18.5°] to [13.7°, 15.8°] when the number of sample increases from 2'000 to 20'000. These ranges correspond to approximately $\pm 30\%$ and $\pm 7\%$ of the median value, respectively.

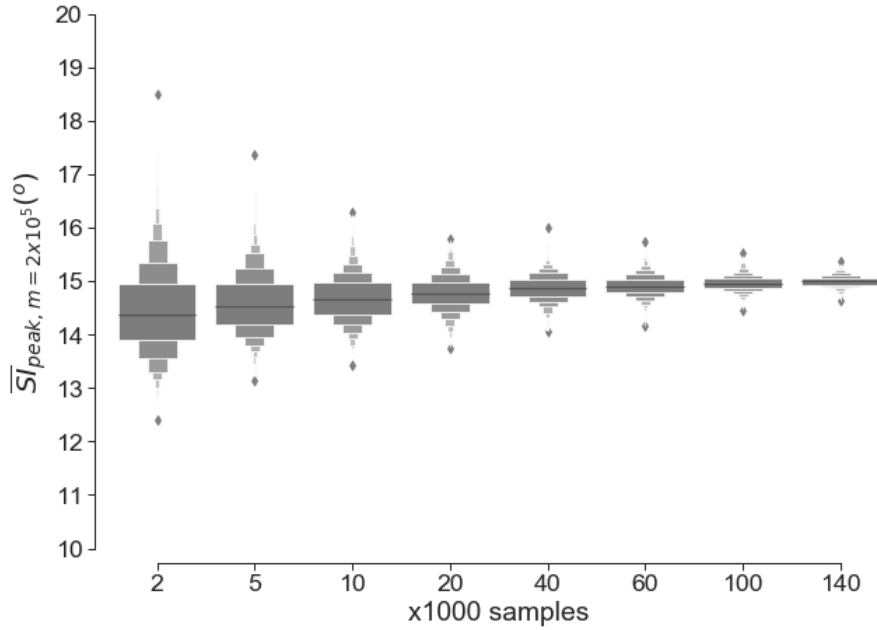


Fig. 3: Letter-value distributions of the prediction of the of swirl intensity for EVT models of shuffled datasets as a function of the number of samples.

It is believed that this method offers a systematic approach to evaluate the trade between the accuracy of extreme value predictions and the length of the available dataset. It statistically compares the EVT models derived from several re-shuffled subsets of data. It is acknowledged however that the availability of at least one long dataset is required to enable this assessment for the observed metric. The convergence of the predictions can be evaluated with the median value of the predictions for the various subset lengths ($\overline{SI}_{peak,m=2 \times 10^5}$). For example, in this case study, $\overline{SI}_{peak,m=2 \times 10^5}$ converges within 0.1° of the measured extreme value $\overline{SI}_{peak,exp} = 15.0^\circ$ with EVT models based on 60 thousand samples respectively (Fig. 4). This disparity of 0.1° is approximately equal to the measurement uncertainty of \overline{SI}_{exp} which has been derived from PIV measurements [9]. Thus, it is inferred that increasing the sample size beyond 60 thousand produces EVT estimates whose disparity from the measured extreme is beyond the uncertainty of the measured variable itself. The range of the predictions obtained with re-shuffles of the samples ($\Delta \overline{SI}_{peak,m=2 \times 10^5}$) can also be used to evaluate the accuracy of the EVT models. $\Delta \overline{SI}_{peak,m=2 \times 10^5}$ sharply reduced from about 6° to 2° when the sample size increased from 5 to 20 thousand (Fig. 4), while $\Delta \overline{SI}_{peak,m=2 \times 10^5}$ further reduced by about 1° when the sample size was increased from 20 to 140 thousand. It can be concluded that, for this case study, it is recommended to consider a sample size between 20 and 60 thousand unsteady \overline{SI}_{exp} measurements to predict the extreme values with an adequate accuracy.

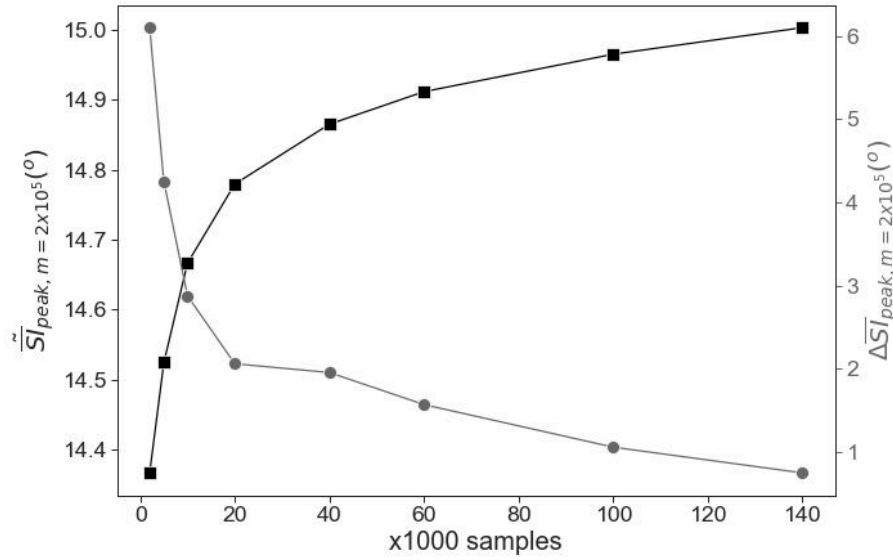


Fig. 4: Convergence of the median value of EVT predictions of shuffled datasets ($\overline{SI}_{peak, m=2 \times 10^5}$) and associated range ($\Delta \overline{SI}_{peak, m=2 \times 10^5}$) in relation to the number of samples.

4. Conclusions

Relative to the industry standard for intake flow distortion evaluation, the contribution of this work is a method to evaluate the required number of observations to predict extreme distortion events with Extreme Value Theory. This work is pertinent to applications in which the duration of the experimental data acquisition for capturing extreme values of unsteady metrics needs to be determined. The method has been used to demonstrate the number of samples needed for reliable extreme value predictions for the swirl distortion in an S-duct intake. It is acknowledged that the distribution of extreme events depends on the unsteadiness of the observations and thus the number of samples will vary depending on the test configuration. However, this work provides a method to make an informed decision on sample length on the in other applications, provided that an initial, sufficiently-large dataset is available. The confidence of the EVT predictions can be informed with the comparison between the median value of the EVT predictions and the measurement uncertainty of the variable, and by considering the range of the EVT predictions relative to the dataset length. The methodology allows users to assess predicted value ranges and select the appropriate sample size for extreme value characterization. It highlights that evaluating variance in estimated extreme values facilitated by shuffling iterations can inform the confidence on the EVT predictions even with limited samples. The envisaged impact of this work is that it can be adopted by the gas turbine engineering community to determine data recording requirement and reduce the costs associated with experimental practice for future assessments. In the case in analysis, the occurrence of random extreme events is that of interest as it could trigger spike-stall inception in compressor fans. Nevertheless, as this method is purely statistical, is it agnostic of the data nature and source. In the context of aero-intake distortion, it is applicable velocity and pressure fluctuations, however this has been already applied to estimate extreme events in material sciences, meteorology, and economics. This is also pertinent for applications similar to the case study where the use of experiments may require a substantial time and cost for the product development and thus require a rational use of resources.

Funding Sources

This work is partially funded by the UKRI, grant reference no. 2202953. The supporting data is not available due to confidentiality agreements.

References

- [1] Breuer, T., and Bissinger, N. C., "Basic Principles - Gas Turbine Compatibility - Gas Turbine Aspects," *Encyclopedia of Aerospace Engineering*, John Wiley & Sons, Ltd, Chichester, UK, 2010.
- [2] Perovic, D., Hall, C. A., and Gunn, E. J., "Stall Inception in a Boundary Layer Ingesting Fan," *Journal of Turbomachinery*, Vol. 141, No. 9, Sep. 2019, doi: 10.1115/1.4043644.
- [3] Kammerer, A., and Abhari, R. S., "Experimental Study on Impeller Blade Vibration During Resonance—Part I: Blade Vibration Due to Inlet Flow Distortion," *Journal of Engineering for Gas Turbines and Power*, Vol. 131, No. 2, Mar. 2009, p. 11, doi: 10.1115/1.2968869.
- [4] Tan, C. S., Day, I., Morris, S., and Wadia, A., "Spike-Type Compressor Stall Inception, Detection, and Control," *Annual Review of Fluid Mechanics*, Vol. 42, No. 1, Jan. 2010, pp. 275–300, doi: 10.1146/annurev-fluid-121108-145603.
- [5] Zhang, W., and Vahdati, M., "A Parametric Study of the Effects of Inlet Distortion on Fan Aerodynamic Stability," *Journal of Turbomachinery*, Vol. 141, No. 1, Jan. 2019, doi: 10.1115/1.4041376.
- [6] Coles, S., "An Introduction to Statistical Modelling of Extreme Values," Springer-Verlag, Bristol, UK, 2001.
- [7] Jacocks, J. L., and Kneile, K. R., "Statistical Prediction of Maximum Time-Variant Inlet Distortion Levels," AEDC-TR-74-121, Arnold Engineering Development Center, Tennessee, US, 1975.
- [8] Tanguy, G., MacManus, D. G., Garnier, E., and Martin, P. G., "Characteristics of unsteady total pressure distortion for a complex aero-engine intake duct," *Aerospace Science and Technology*, Vol. 78, Jul. 2018, pp. 297–311, doi: 10.1016/j.ast.2018.04.031.
- [9] Migliorini, M., Zachos, P. K., MacManus, D. G., and Haladuda, P., "S-duct flow distortion with non-uniform inlet conditions," *Proceedings of the Institution of Mechanical Engineers, Part G: Journal of Aerospace Engineering*, May 2022, p. 095441002211016, doi: 10.1177/09544100221101669.
- [10] "Distortion Synthesis/Estimation Techniques," Aerospace Information Report AIR 5826B, Society of Automotive Engineers, 2017.
- [11] Zachos, P. K., MacManus, D. G., Prieto, D. G., and Chiereghin, N., "Flow Distortion Measurements in Convolved Aeroengine Intakes," *AIAA Journal*, Vol. 54, No. 9, Sep. 2016, pp. 2819–2832, doi: 10.2514/1.J054904.
- [12] "A Methodology for Assessing Inlet Swirl Distortion," Aerospace Information Report AIR 5686, Society of Automotive Engineers, Warrendale, PA, 2017.
- [13] MacManus, D. G., Chiereghin, N., Prieto, D. G., and Zachos, P., "Complex Aeroengine Intake Ducts and Dynamic Distortion," *AIAA Journal*, Vol. 55, No. 7, Jul. 2017, pp. 2395–2409, doi: 10.2514/1.J054905.
- [14] Gil-Prieto, D., MacManus, D. G., Zachos, P. K., and Bautista, A., "Assessment methods for unsteady flow distortion in aero-engine intakes," *Aerospace Science and Technology*, Vol. 72, Jan. 2018, pp. 292–304, doi: 10.1016/j.ast.2017.10.029.
- [15] Gil-Prieto, D., Zachos, P. K., MacManus, D. G., and McLelland, G., "Unsteady Characteristics of S-duct Intake Flow Distortion," *Aerospace Science and Technology*, Vol. 84, No. 1, Jan. 2019, pp. 938–952, doi: 10.1016/j.ast.2018.10.020.
- [16] Mehdi, A., "Effect of Swirl Distortion on Gas Turbine Operability," Propulsion Engineering Centre, School of Aerospace, Transport and Manufacturing, Cranfield University, 2014.
- [17] Bayer, D., and Diaconis, P., "Trailing the Dovetail Shuffle to its Lair," *The Annals of Applied Probability*, Vol. 2, No. 2, May 1992, doi: 10.1214/aoap/1177005705.
- [18] Hofmann, H., Wickham, H., and Kafadar, K., "Letter-Value Plots: Boxplots for Large Data," *Journal of Computational and Graphical Statistics*, Vol. 26, No. 3, Jul. 2017, pp. 469–477, doi: 10.1080/10618600.2017.1305277.

Evaluation of extreme value predictions for unsteady flow distortion of aero-engine intakes

Migliorini, Matteo

2024-02-13

Attribution 4.0 International

Migliorini M, Zachos PK, MacManus DG. (2024) Evaluation of extreme value predictions for unsteady flow distortion of aero-engine intakes. *Journal of Engineering for Gas Turbines and Power*, Volume 146, Issue 9, September 2024. Paper number GTP-23-1520

<https://doi.org/10.1115/1.4064728>

Downloaded from CERES Research Repository, Cranfield University